# Short-chain fatty acid acetate triggers antiviral response mediated by RIG-I in cells from infants with respiratory syncytial virus bronchiolitis

Krist H. Antunes,[a] Renato T. Stein,[b,*] Caroline Franceschina,[a] Emanuelle F. da Silva,[a] Deise N. de Freitas,[a] Josiane Silveira,[a] Magáli Mocellin,[a] Lidiane Leitão,[a] José L. Fachi,[c] Laís P. Pral,[c] Amanda Gonzalez,[a] Sarah Oliveira,[c] Leonardo Duarte,[a] Gisele Cassão,[a] João I.B. Gonçalves,[a] Tatiane M. Reis,[a] Bruno L Abbadi,[d] Maiele Dornelles,[d] Nathália D.M. Sperotto,[d] Maurício Rigo,[a] Hosana Rodrigues,[e] Marcus Jones,[b] Matias Epifanio,[b] Suzana Guima,[f] João C. Setubal,[f] Taissa R. Jorge,[g] Daniel S. Mansur,[g] Fabiana Q. Mayer,[h] Ana Paula M. Varela,[h] Cristiano V. Bizarro,[d] Pablo Machado,[d] Luiz A. Basso,[d] Fernando P. Polack,[i] Adnan Custovic,[j] Marco A.R. Vinolo,[b,1,*] and Ana Paula D. de Souza[a,1,*]

[a]Laboratory of Clinical and Experimental Immunology, Health and Life Science School - Pontifical Catholic University of Rio Grande do Sul, Porto Alegre, Rio Grande do Sul 90610-000, Brazil
[b]Department of Pediatrics, School of Medicine, PUCRS, São Lucas Hospital PUCRS, Porto Alegre, Rio Grande do Sul 90610-000, Brazil
[c]Laboratory of Immunoinflammation, Department of Genetics, Evolution, Microbiology and Immunology - Institute of Biology, University of Campinas, Campinas, São Paulo 13083-862, Brazil
[d]Centro de Pesquisas em Biologia Molecular e Funcional (CPBMF), Pontifical Catholic University of Rio Grande do Sul, Porto Alegre, Brazil
[e]Laboratory of Nutritional Genomics, School of Applied Sciences, University of Campinas, Limeira, São Paulo, Brazil
[f]Department of Biochemistry, Chemistry Institute, University of São Paulo, São Paulo, São Paulo, Brazil
[g]Laboratory of Imunobiology, Department of Microbiology, Immunology and Parasitology, Universidade Federal de Santa Catarina, Florianópolis, Santa Catarina, Brazil
[h]Molecular Biology Laboratory, Veterinary Research Institute Desidério Finamor, Agricultural Diagnosis and Research Department, Secretariat of Agriculture, Livestock and Irrigation, Eldorado do Sul, Rio Grande do Sul, Brazil
[i]Fundación Infant, Buenos Aires, Argentina
[j]National Heart and Lung Institute, Imperial College London, UK

## Summary

**Background** Gut microbiota-derived short-chain fatty-acid (SFCA) acetate protects mice against RSV A2 strain infection by increasing interferon-β production and expression of interferon-stimulated genes (*ISGs*). However, the role of SFCA in RSV infection using strains isolated from patients is unknown.

**Methods** We first used RSV clinical strains isolated from infants hospitalized with RSV bronchiolitis to investigate the effects of *in vitro* SCFA-acetate treatment of human pulmonary epithelial cells. We next examined whether SCFA-acetate treatment is beneficial in a mouse model of RSV infection using clinical isolates. We sought to investigate the relationship of gut microbiota and fecal acetate with disease severity among infants hospitalized with RSV bronchiolitis, and whether treating their respiratory epithelial cells with SCFA-acetate *ex-vivo* impacts viral load and *ISG* expression. We further treated epithelial cells from SARS-CoV-2 infected patients with SCFA-acetate.

**Findings** *In vitro* pre-treatment of A549 cells with SCFA-acetate reduced RSV infection with clinical isolates and increased the expression of RIG-I and *ISG15*. Animals treated with SCFA-acetate intranasally recovered significantly faster, with reduction in the RSV clinical isolates viral load, and increased lung expression of *IFNB1* and the RIG-I. Experiments in RIG-I knockout A549 cells demonstrated that the protection relies on RIG-I presence. Gut microbial profile was associated with bronchiolitis severity and with acetate in stool. Increased SCFA-acetate levels were associated with increasing oxygen saturation at admission, and shorter duration of fever. *Ex-vivo* treatment of patients' respiratory cells with SCFA-acetate reduced RSV load and increased expression of ISGs *OAS1* and *ISG15*, and virus recognition receptors MAVS and RIG-I, but not *IFNB1*. These SCFA-acetate effects were not found on cells from SARS-CoV-2 infected patients.

**eBioMedicine 2022;77: 103891**
Published online 24 February 2022
https://doi.org/10.1016/j.ebiom.2022.103891

*Corresponding authors.
*E-mail addresses:* rstein@pucrs.br (R.T. Stein), mvinolo@g.unicamp.br (M.A.R. Vinolo), ana.duarte@pucrs.br (A.P.D. de Souza).

[1] These authors contributed equally to this work.

**Interpretation** SCFA-acetate reduces the severity of RSV infection and RSV viral load through modulation of RIG-I expression.

**Funding** FAPERGS (FAPERGS/MS/CNPq/SESRS no. 03/2017 - PPSUS 17/2551-0001380-8 and COVID-19 20/2551-0000258-6); CNPq 312504/2017-9; CAPES) - Finance Code 001.



**Keywords:** Acetate; Respiratory syncytial virus; Clinical isolates; RIG-I

## Research in context

### *Evidence before this study*

Our group has recently published a study demonstrating the protective role of SCFA-acetate treatment in disease caused by RSV. This protective mechanism is associated with the increase in antiviral activity in a way that is dependent on IFNAR and GPR43. However, other molecules that could be involved in this antiviral mechanism have not been investigated. Furthermore, the action of SCFA-acetate on infection caused by a non-laboratory strain of RSV has not yet been explored. We then researched in PubMed for terms "human, respiratory virus", "acetate", "fatty acid, short-chain", "interferon", "antiviral response", and "bronchiolitis". We did not find published studies with the same or similar proposal that we had aimed for with this study.

### *Added value of this study*

We show that SCFA-acetate treatment against RSV strains isolated from patients on human pulmonary epithelial cell line reduced viral load depending on RIG-I presence. We also observe in a mouse model, where animals treated with SCFA-acetate intranasally after infection recovered significantly faster, with a significant reduction in the RSV clinical isolates' viral load in the lung, and increased lung expression of *Ifnb1* and RIG-I. We further describe that ex-vivo treatment of our patients' respiratory cells with SCFA-acetate significantly reduces RSV load. RIG-I has shown consistently to be an acetate-modulated molecule in all analyses performed. We describe that the gut microbiota profile in infants is associated with bronchiolitis severity and with short-chain fatty acids (SFCA) levels measured in the stool. Interestingly, we observed that higher levels of the SCFA acetate is significantly associated with increased oxygen saturation at the time of hospital admission, and with a shorter duration of fever. We also observed the effect of SCFA-acetate on SARS-CoV-2 infection which the performance is different from what we found with RSV.

### *Implications of all the available evidence*

We believe that these findings support the concept that low-cost and natural product from gut microbiota may have a role controlling severe RSV infection direct on the respiratory tract.

## Introduction

Respiratory syncytial virus (RSV) is an important cause of lower respiratory tract infection (LRTI) in infants and is associated with approximately 100,000 deaths per year globally.[1,2] Despite advances in active and passive immunization,[3] no effective therapy or vaccine is yet available.[4,5] RSV infection is ubiquitous and by the age of 2 years most children are infected.[1] The clinical presentation of RSV disease is highly heterogeneous, ranging from asymptomatic infection or mild upper respiratory illness, to severe and sometimes fatal LRTI. It is estimated that 5–10% of the infected children may require hospitalization, and these marked differences in clinical presentation are likely related to the heterogeneity in underlying mechanisms.[6,7]

Risk factors associated with severe RSV disease include prematurity, male gender, environmental exposures[8] and low early-life lung function (likely associated with structural characteristics and size of the airways[9]). The innate immune response is involved in initial virus recognition,[10] and type I interferons (IFN-$\alpha$ and IFN-$\beta$) are key mediators inducing apoptosis of virus-infected cells and over 300 IFN-stimulated genes (ISGs), many of which have multiple direct anti-viral activities.[11] Through these combined effects, type I IFNs can abort virus replication in infected cells.[12] However, RSV can subvert the antiviral response by decreasing the induction type I IFNs.[13,14] Non-structural protein NS1 and NS2 suppress IFNs production by binding to mitochondrial antiviral-signaling protein (MAVS) which disrupts the MAVS-RIG-I interaction required for IFN production.[15] The majority of the data exploring the antiviral mechanism against RSV are obtained using the laboratory strain (A2 or Long). Molecular epidemiology studies have provided convincing evidence of antigenic and sequence variability among RSV laboratory strains and isolates.[16–18] Therefore, it is central to investigate those mechanisms through RSV strain isolated from patients.

Altered gut microbiota is associated with the severity of RSV disease,[19–21] and gut microbiome may impact upon the development and maturation of antiviral responses.[22,23] Our group has recently demonstrated in an experimental model that treatment with the gut microbiota-derived short-chain fatty acid (SCFA) acetate protects mice against RSV A2 infection by increasing IFN-$\beta$ production and expression of *ISGs* in the lungs.[24] To determine whether clinical strains of RSV also increase IFN-$\beta$ production and expression of ISGs upon SCFA-acetate treatment we used RSV clinical strains isolated from infants hospitalized with RSV bronchiolitis and we ascertained the antiviral effect of SCFA-acetate in different approaches. We found that pre-treatment with SCFA-acetate protects against RSV clinical strains infection *in vitro*, and this effect relies on RIG-I presence. Through a translational approach we have identified that using SCFA-acetate as a treatment following RSV infection is beneficial in an *in vivo* mouse model. We then proceeded to investigate whether treating respiratory epithelial cells isolated from patients with RSV bronchiolitis with SCFA-acetate impact upon RSV viral load and *ISG* expression. We probed the mechanisms by which SCFA-acetate protect against RSV infection which is different from SARS-CoV-2 infection.

## Methods

### Isolation of clinical RSV strains

Nasopharyngeal aspirate samples from 2 patients were diluted in 5 ml of DMEM low glucose containing 1000 µg/mL of gentamycin and inoculated into culture of Vero cells. After 1h incubation at 37 °C for complete viral adsorption, the viral inoculum was removed and added 10 ml of Opti-MEM supplemented with 2% of FBS and 1000 µg/mL of gentamycin into the flask. The culture was kept in an incubator at 37 °C and 5% $CO_2$ until macro-visualization of the viral cytopathic effect on the cells. Cells were harvested, centrifuged and the cell pellet was subjected to freeze-thaw cycles to obtain new viral particles. Afterwards, the viral aliquots were given sucrose cryoprotector and then stored in -80 °C until titration or further analysis. Viral titration was determined by plaque-forming unit (PFU) assay, using anti-RSV antibody (Millipore Cat# AB1128, RRID: AB_90477). The antigenic subgroup was identified by real-time PCR targeting the expression of the following primers and probes: Vi99990014_p0 (RSV A) and Vi99990015_p0 (RSV B) (ThermoFisher Scientific Cat# A39420). The viral nomenclature was made based on antigenic subgroup-city of isolation/strain number/year (RSV B-POA10/2018 and RSV A-POA43/2018).

### *In vitro* analysis

Mycoplasma-free wild-type, *RIG-I* or *IFNAR1* knockout A549 cells generated by CRISPR-Cas9 (ATCC Cat# CCL-185, RRID: CVCL_0023) were used for *in vitro* analysis. Cells were pre-treated with 260 µM of SCFA-acetate for 24 h, concentration that worked best against *in vitro* RSV infection previously.[24] Cells were infected with $10^4$ PFU/ml (0.5 MOI) of the two RSV isolates for further 24 h or 4 days. Cells were harvested 24 h or 4 days after infection and processed for RNA extraction and cDNA syntheses. IFN-$\beta$ and ISGs expression were assessed by real-time PCR. We measured cell death and viability by propidium iodide staining using flow cytometry, and viral loads were accessed by real time PCR.

For SARS-CoV-2 *in vitro* analysis, mycoplasma-free Calu-3 cells (ATCC Cat# HTB-55, RRID: CVCL_0609) were pre-treated with 200 µM or 400 µM of SCFA-acetate for 24 h. These cells were chosen due to its high capacity to express ACE2 and TMPRSS2, facilitating virus replication.[25–27] Cells were infected with 0.1 MOI of SARS-CoV-2 (Brazilian clinical isolate virus HIAE-02-SARS-CoV-2/SP02/human/2020/bra (GenBank MT126808) kindly donated by Prof. Dr. Edison Durigon (ICB-USP) for further 24 h or 4 days. Cells were harvested for RNA extraction and cDNA syntheses. Real-time PCR of viral load was performed using N1 SARS target genes and RNAseP as endogenous control.

### Real-time PCR of *in vitro* analysis

Samples in RNA later were thawed and centrifuged. Supernatant was discarded and the pellet was subjected to the RNA extraction protocol using TRIzol® reagent (Thermo Fisher Scientific, Waltham, MA, USA) following the manufacturer's instructions. Complementary DNA (cDNA) was synthesized from the extracted total RNA using the GoScript® Reverse Transcription Kit (Promega®, Madison, WI, USA). cDNA samples were stored at -20 °C until PCR analysis. Real-time PCR analyzes were performed using 4 ng of a cDNA sample. The quality of the cDNA for each patient was tested by endogenous $\beta$-actin gene amplification using TaqMan-specific primers and probes (Hs01060665_g1 ACTB, Thermo Fisher Scientific). The RSV viral load was accessed by RSV F protein gene expression using the indicated specific primers and probes: forward primer-5′-AACAGATGTAAGCAGCTCCGTTATC-3′, reverse primer- 5′-GATTTTTATTGGATGCTGTACATTT-3′ and probe- 5′ FAM/TGCCATAGCATGACA-CAATGGCTCCT-TAMRA/-3'. The relative expression of the IFN-$\beta$, ISG15 and OAS1 gene was accessed using primers and probes for TaqMan Assay (Hs01077958_s1 *IFNB1*; Hs01921425_s1 *ISG15*; Hs00973635_m1 *OAS1*, Thermo Fisher Scientific). The gene expression of GAPDH, ISGs, TLR4 and FFAR2 was accessed using the following primer sets: *GAPDH* (forward primer: 5'-GGAGCGAGATCCCTCCAAAAT-3', reverse primer: 5'-GGCTGTTGTCATACTTCTCATGG-3'); RIG-I (*DDX58* gene) (forward primer: 5'-CACCTCAGTTGCT-GATGAAGGC-3', reverse primer: 5'-

GTCAGAAGGAAGCACTTGCTACC-3'); *MAVS* (forward primer: 5'-GTCACTTCCTGCTGAGA-3', reverse primer: 5'-TGCTCTGAATTCTCTCCT-3'); *TLR4* (forward primer: 5'-TGGTGTCCCAGCACTTCATC-3', reverse primer: 5'-CTGTCCTCCCACTCCAGGTA-3'); *FFAR2* (forward primer: 5'-GGCTGCGTCGAACTTCCGCT-3', reverse primer: 5'-GCCAAAACTCGTGAGGGCGC-3'). PCR conditions followed the GoTaq™ Probe qPCR Master Mix (Promega™, Madison, WI, USA) or SYBR Green/ROX qPCR Master Mix protocols (Thermo Fisher Scientific, Waltham, MA, USA). Quantification of gene expression was conducted using StepOne™ (Applied Biosystems). The threshold cycle value (ΔCt) was obtained subtracting the Ct value from the endogenous gene by the Ct value of the target gene. The gene expression was calculated according to 2-ΔCt formula.

### Western blotting analysis

Protein samples were separated on 10% SDS-page polyacrylamide gels and transferred to nitrocellulose membrane (Bio-rad). Then the membrane was stained with Anti-RIG-I/DDX58 polyclonal antibody (Sigma-Aldrich Cat# SAB5700643, RRID: AB_11203763), mouse β-actin monoclonal antibody (Sigma-Aldrich Cat# A2228, RRID: AB_476697). For the protein quantification, ImageJ software was used. β-actin was used to normalize protein quantification. The full blots image is available in Supplemental Western blots.

### Immunofluorescence analysis

Slides were fixed with PBS 1 × 0.5% Triton X-100 for 20 min and incubated with Fc Block (supernatant of 2.4G2 cells with 5% heat-inactivated human serum) for an additional 20 min. Cells were stained with 1:500 of goat anti-RSV antibody (Millipore Cat# AB1128, RRID: AB_90477) followed by 1:1000 of secondary rabbit anti-goat IgG (H + L)-HRP (Santa Cruz Biotechnology Cat# sc-2922, RRID: AB_656965) antibody. Antibody dilutions and washes were performed in 1X PBS. Nuclear staining was performed with Hoechst 33342 (ThermoFisher Scientific), and slides were mounted with glycerin for analysis under a fluorescence microscope (Olympus). Images were acquired using CellSens software (Olympus). Fluorescence intensity and quantification were measured using ImageJ.

### *In vivo* analysis

We investigated the effect of treatment with SCFA-acetate on RSV infection *in vivo* using 6–8-week-old female BALB/cJ mice. Mice were anesthetized with 5% isoflurane and infected intranasally with $10^7$ PFU/ml of RSV A-POA43/2018 clinical isolate. Starting 24 h after the infection, animals were treated intranasally with 20 mM of SCFA-acetate daily for 4 days. We choose to test this concentration based on the study of Thio et al.[28] PBS was administered intranasally in the control group. All animals were weighed daily. Data analysis was performed 5 days post infection. Bronchoalveolar lavage fluid (BALF) was collected to ascertain cells count; the left lung was removed for either gene expression analysis or viral plaque assay. Mice were housed at the Animal Facility of the Institute of Biology, University of Campinas. All animal procedures were performed in accordance with protocols approved by CEUA/UNICAMP (protocols 4022-1 and 4599-1). The ARRIVE guidelines (Animal Research: Reporting of *in vivo* Experiments) checklist was followed during the planning, the conduction, and the writing of this study.

### Real time PCR in mouse lung tissue

Total lung RNA was extracted, and cDNA was synthesized as described above. To accesses IFN-β expression primers and probes for TaqMan Assay were used (Mm00439552_s1 *Ifnb1*) and mouse β-actin (Mm02619580_g1 *Actb*) was employed as an endogenous control gene. For the ISG expression, the following primer sets were used: *Oas1* (forward primer: 5'-AAAAGGAGGAGCCATGGCAGT-3' reverse primer: 5'-CTGAGCCCAAGGTCCATCAG-3');

*Isg15* (forward primer: 5'-GAGCTAGAGCCTGCAGCAAT-3' reverse primer: 5'-TCACGGACACCAGGAAATCG-3'); *Mavs* (forward primer: 5'-TCTCTTGTCCATCTCAGTCCA-3', reverse primer: 5'-TTCCCGATCTGCCTGTAGGA-3'); RIG-I (*Ddx58* gene) (forward primer: 5'-CACTGTCCTTGGAGACGCTT-3', reverse primer: 5'- GGTTCTGAACTCCGCTCACA-3'); *B2m* (forward primer: 5'-CCCCAGTGAGACTGATACATACG' reverse primer: 5'-CGATCCCAGTAGACGGTCTTG').

PCR conditions followed the GoTaq™ Probe qPCR Master Mix (Promega™, Madison, WI, USA) or SYBR Green/ROX qPCR Master Mix protocols (Thermo Fisher Scientific, Waltham, MA, USA). The 2-ΔCt analysis was used to calculate the gene expression.

### Lung histology

The left lung was embedded in paraffin blocks, cut into 5 μm sections, and stained with H&E to identify cellular infiltrate. Slide analysis was performed in a blinded manner.

### Human data

This was a cross-sectional study. The study was conducted in the São Lucas Hospital, at Pontifical Catholic University of Rio Grande do Sul (PUCRS), Rio Grande do Sul, Brazil. We recruited children under 12 months of age who were hospitalized with RSV-confirmed bronchiolitis. Subjects with comorbidities or using inhaled corticosteroids were excluded (see flowchart in the Supplemental Methods). Respiratory viruses (RSV,

influenza, parainfluenza virus types I, II, III, adenovirus) were detected using a direct immunofluorescence assay in nasopharyngeal aspirates collected within 24 h of hospitalization. We recruited infants who were positive for RSV and negative for all other viruses.

We used the length of hospitalization, oxygen saturation at the time of admission, and duration of symptoms (wheezing, fever, cough, nasal congestion), previously described as markers of bronchiolitis severity.[29–31] Information on demographics and medical history was collected using validated questionnaires.

For COVID-19 analysis we recruited adult patients between 18 and 67 years old with positive RT-PCR for SARS-CoV-2 within 3 weeks of the onset of symptoms. We excluded patients on corticosteroid treatment; pregnant or lactating women; patients with severe liver disease (alanine aminotransferase and/or aspartate aminotransferase > 5x above normal); severe nephropathy (kidney transplant or dialysis), HIV infection, cancer, hereditary angioedema, other immunodeficiencies, past myocardial ischemic disease, past thromboembolic disease. A total of 13 patients were included in the study (Supplementary Table E1).

### Stool collection

Stools were collected in diapers by the mother within the first 48 h of hospitalization. Approximately 5 g of feces were collected with the aid of a disposable spatula and stored in an identified collection pot and then placed immediately in a -80 °C freezer until analysis.

### Sequencing of DNA from microbiota bacteria

Stool samples were thawed, and the bacterial DNA were extracted and purified using the QIAamp DNA stool mini kit (Qiagen, Hilden, Germany) following the manufacturer's instructions. The 16S rRNa amplicons were generated by PCR with primers targeting the V2 region of the gene using a Pfx polymerase enzyme (Thermo Fisher Scientific, Waltham, MA, USA). The primers were designed with Illuminas©' adapters. Amplicons were purified with AMPure beads and sequenced using a Miseq v2 500 cycle reagent kit, which generates paired end reads of 250 bp, in a Miseq equipment (Illumina, San Diego, CA, USA).

### SCFA quantification

Stool samples were thawed (about 1 g) and homogenized with extraction buffer (1.0% $H_3PO_4$, 0.1% $HgCl_2$). 10 mg of citric acid, 20 mg of NaCl, 20 $\mu$L of 0.1N HCl, 100 $\mu$L of feces pellet, and 100 $\mu$L of butanol solvent were added to a 1.5 ml microtube. 20 uL of internal standard, caprylic acid, a solution of 0.5 mg/ml in H2O was further instilled in the tubes. Samples were homogenized for 1 min to form an emulsion appearance in the solution. They were centrifuged for 10 min at 12000 rpm, room temperature. The phases were separated, and the organic phase of the solution was collected and placed in vials for GC 2010 gas chromatograph analysis (Shimadzu, Kyoto, Japan) using N2 as the entrainer gas.

### *Ex vivo* treatment of airway cells with SCFA-acetate

Nasopharyngeal aspirates samples were diluted in 1x PBS buffer saline and 0.5 mM EDTA solution and centrifuged to obtain the cells. The cells were suspended in RPMI 1640 medium (Gibco™, Thermo Fisher Scientific, Waltham, MA, USA) supplemented with 2% inactivated fetal bovine serum (FBS) (Cultilab, Campinas, SP, Brazil). Cells from each patient were then placed in a 96-well plate, receiving or not treatment with SCFA-acetate (260 $\mu$M) for 24 h. The culture was kept in an incubator with 5% $CO_2$ at 37 °C. Cells were then harvested and kept in RNA-stabilizing solution (RNA later, Thermo Fisher Scientific, Waltham, MA, USA) at -80 °C until RNA extraction. Similarly, nasopharyngeal aspirate samples from patients with COVID-19 were cultured for 24 h in the presence of SCFA-acetate. The SARS-CoV-2 viral titer was measure by viral plaque assay (Plaque-forming units (PFU)/ml).

### Real-time PCR of *ex vivo* analysis

RNA was extracted using TRIzol® reagent (Thermo Fisher Scientific, Waltham, MA, USA) following the manufacturer's instructions. Complementary DNA (cDNA) was synthesized from the extracted total RNA using the GoScript® Reverse Transcription Kit (Promega®, Madison, WI, USA). cDNA samples were stored at -20 °C until PCR analysis. Real-time PCR analyses were performed using 8 ng of cDNA. The quality of the cDNA for each patient was tested by endogenous $\beta$-actin gene amplification using TaqMan-specific primers and probes (Hs01060665_g1 *ACTB*, Thermo Fisher Scientific). The RSV load was accessed by RSV F-protein gene expression. Specific primers and probes are listed above in this section at *in vitro* analysis. Quantification of ISG expression was conducted using StepOne™ (Applied Biosystems). The threshold cycle value (ΔCt) was obtained subtracting the Ct value from the endogenous gene by the Ct value of the target gene. The gene expression was calculated according to $2^{-\Delta Ct}$ formula.

### Ethics

All animal experiments were performed in accordance with Animals Act 1986 and the ARRIVE guidelines following protocols approved by CEUA/UNICAMP (protocols 4022-1 and 4599-1). For infant study, the Institutional Review Boards of PUCRS (Brazil) approved the protocol (approval number 70271517.6.0000.5336), and the study conformed to standards indicated by the Declaration of Helsinki.

Informed consent was obtained from the parents of each enrolled infant. For the COVID-19 study The Institutional Review Boards of PUCRS approved the protocol (approval number 30754220.3.0000.5336); written informed consent was obtained from the patients.

### Statistical analysis

As there was no data in the literature that verify the SCFA levels as an outcome in respiratory infections, which allows a sample calculation based on the mean and standard deviation of two groups, severe and non-severe, we decided to base our study on the prevalence of RSV infection in our institution and recruit all patients who met the inclusion criteria. A study carried out by our research group at the same hospital where this study took place recruited 184 patients in two years of collection (two winters) and identified 56.5% of patients positive for RSV.[32] The same study identified a mean age of 3 months.[32] Based on this and the fact that data would be collected in just one year (one winter), we aimed to recruit 52 RSV positive patients, which was not possible due to our exclusion criteria (mainly the use of antibiotics), reducing the sample size for 30 patients.

The data were summarized as median and interquartile range (IQR) or mean and standard error of the mean (SEM). Univariate comparisons between groups were performed using the Student *t*-test, Mann-Whitney test, chi-square test, Wilcoxon test, one-way ANOVA and Kruskal-Wallis for multiple comparisons (with Dunn's multiple comparison test as post hoc). The data were analyzed using IBM SPSS Statistics Version 25.0 (IBM Corp, NY, USA) and GraphPad Prism Version 8.0 (GraphPad Software, CA, USA).

### Role of Funders

The Funders did not have any role in study design, data collection, data analyses, interpretation, or writing of report.

## Results

### Pre-treatment with SCFA-acetate protects against RSV infection in a RIG-I-dependent manner

Infections with different strains of RSV can result in a distinct pathology.[18] To test whether SCFA-acetate has any effect on viral infection caused by a virus other than the laboratory strain, we isolated two RSV clinical strains from infants with bronchiolitis. The two RSV isolates were then characterized by their gene expression identifying subgroups A and B as RSV-A (A-POA43/2018) and RSV-B (B-POA10/2018). *In vitro* pre-treatment of human pulmonary epithelial cells (A549) with acetate prevented cell death caused by RSV infection (Figure 1, a–f), and reduced viral load in human epithelial pulmonary lines infected with either RSV isolates (Figure 1, g,h). We used the same SCFA-acetate concentration tested with RSV A2 strain.[24] Furthermore, SCFA-acetate diminished RSV replication in these cells (Figure 1, h–j). SCFA-SCFA-acetate pre-treatment increased the expression of *ISG15* in response to RSV infection, but not *IFNB1* or *OAS1* expression (Figure 1, k–m) during A-POA43/2018 infection. Also, SCFA-acetate increased the expression of *MAVS*, MDA5 (*IFIH1*), and RIG-I (*DDX58*), important viral sensor and antiviral molecules (Figure 1, n–p). Type III interferons are also important for controlling RSV infection in epithelial cells.[33] However, SCFA-acetate did not modulate IFN$\lambda$ during infection with clinical strains of RSV (Figure 1, q). Intrigued by the fact that SCFA-acetate could be acting not only on gene expression, but also on post-translational outcome, we investigated the RIG-I protein amount. In line with the gene expression results, RIG-I protein production was also increased by SCFA-acetate treatment during RSV infection (Figure 1, r, s). SCFA-acetate treatment alone did not induce RIG-I at 24 h after infection. These data suggest that SCFA-acetate pre-treatment does play a role in protecting from RSV clinical isolates infection through increasing antiviral response.

Based on our findings that SCFA-acetate treatment modulates RIG-I expression in the pulmonary epithelial cells, we proceeded to test whether this molecule is involved in the SCFA-acetate protective mechanism against RSV. To test this, we used CRISPR/Cas9 A459 RIG-I knockout cells (*RIG-I* KO, Figure 2) and infected them with the two RSV clinical isolates. SCFA-acetate did not protect against cell death caused by the infection of both clinical isolates in the absence of RIG-I (Figure 2, a, b). Moreover, the lack of RIG-I impaired the capacity of SCFA-acetate to reduce virus replication and expression in these cells (Figure 2, c–e). The noticed effect was not only limited to infection by the clinical isolates, but also to infection by laboratory virus strain A2 (Figure 2, f, g). To investigate whether RIG-I is acting as an ISG in this context, we pre-treated A549 IFNAR1 knockout cells with SCFA-acetate and then infected with the two RSV clinical isolates. Increased expression of RIG-I was dependent on IFNAR1 expression. (Figure 2, h). Also, SCFA-acetate did not have the same effect on reducing the viral load in the absence of IFNAR (Figure 2, i). Together these findings point to a possible role of RIG-I acting as an ISG, and a key component to control RSV replication.

### Intranasal SCFA-acetate treatment following RSV infection is effective against the disease

To pursue a more translational and therapeutical approach, we decided for an *in vivo* method of infection with the RSV isolates, where we performed the SCFA-acetate treatment intranasally (i.n.) following RSV

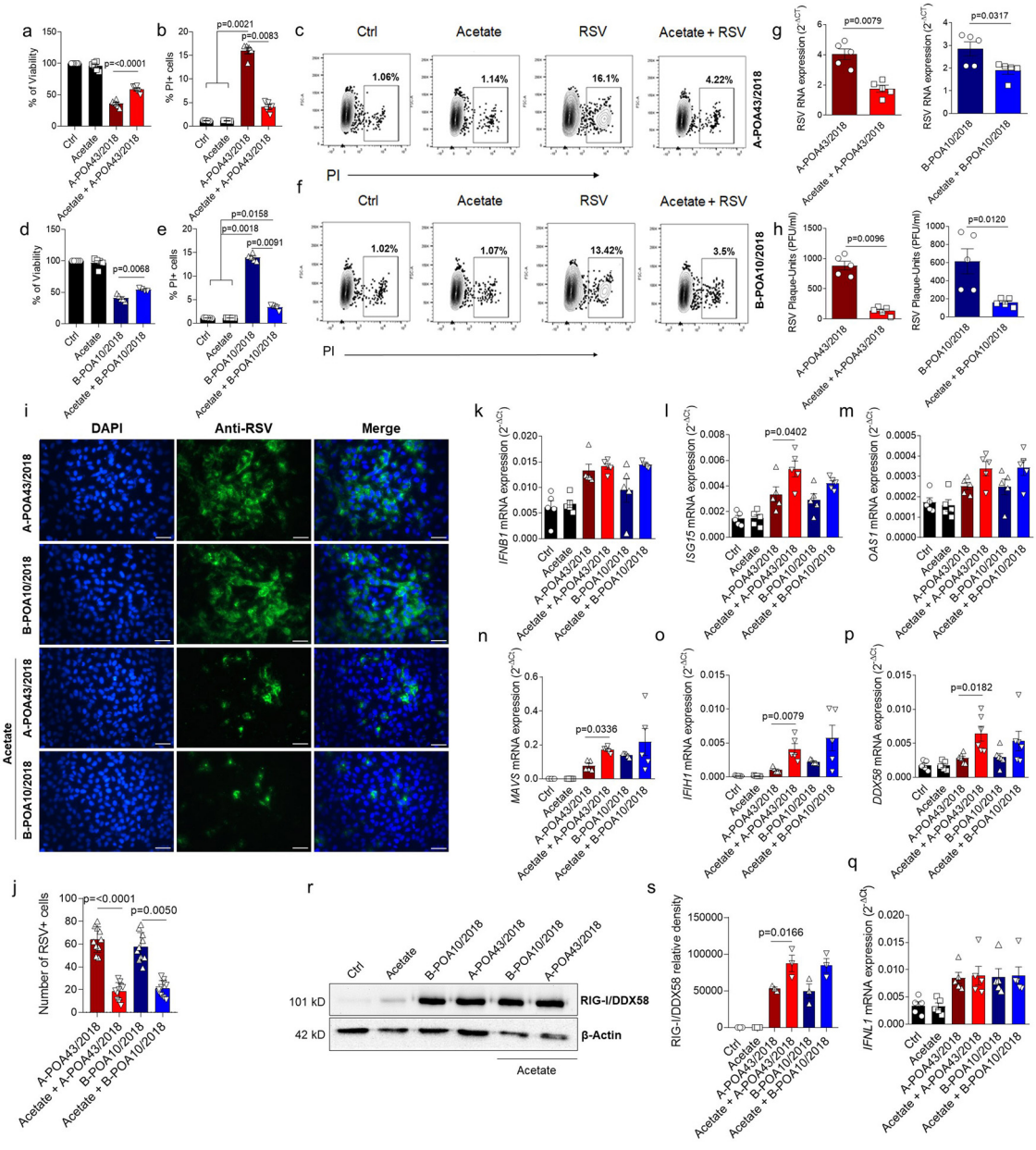


**Figure 1.** Acetate protects against RSV clinical isolate infection in human pulmonary cells. a, A549 cells were pre-treated with 260 µM of acetate for 24 h and infected with $10^4$ PFU/ml of clinical isolate RSV A-POA43/2018 or B-POA10/2018 for 96 h (a−j) or 24 h (q−s). a and c, Percent of cell viability measured by MTT assay (using untreated/uninfected cells as viability control). b and e, Percent of PI (propidium iodide) positive cells detected by flow cytometry. c and f, Representative FACS profile of PI positive cells. Gating strategy is shown in Supplementary Fig. E4 3. g, RSV F protein RNA levels detected using real-time PCR ($2^{-\Delta Ct}$). h, Viral load measured by Plaque-forming unit (PFU) using specific RSV antibody. i, Fluorescence images of RSV (green) and cell nuclei using Hoescht (blue). Third panel shows data co-localization (merge). Scale bars = 60 µm. j, Immunofluorescence quantification measured by the number of RSV positive (green) cells. k-q, *IFNB1*, *ISG15*, *OAS1*, *MAVS*, *IFIH1*, *DDX58* (RIG-I) and *IFNL1* gene expression detected by real-time PCR ($2^{-\Delta Ct}$). r, Western blot analysis of RIG-I/DDX58 and $\beta$-actin in the whole cell. The whole blot image is available on Supplementary Fig. 5. s, Protein bands quantification. Graphic shows data normalized by $\beta$-actin. Data are presented as mean ± SEM. All the experiments were performed in quadruplicates. Data are representative of 3 independent experiments, except in *r* and *s*, where 2 independent experiments were performed. Statistical significance between groups was determined with Kruskal−Wallis, except in G and H, in which Mann−Whitney was used. A *p*-value lower than 0.05 was considered as significative.

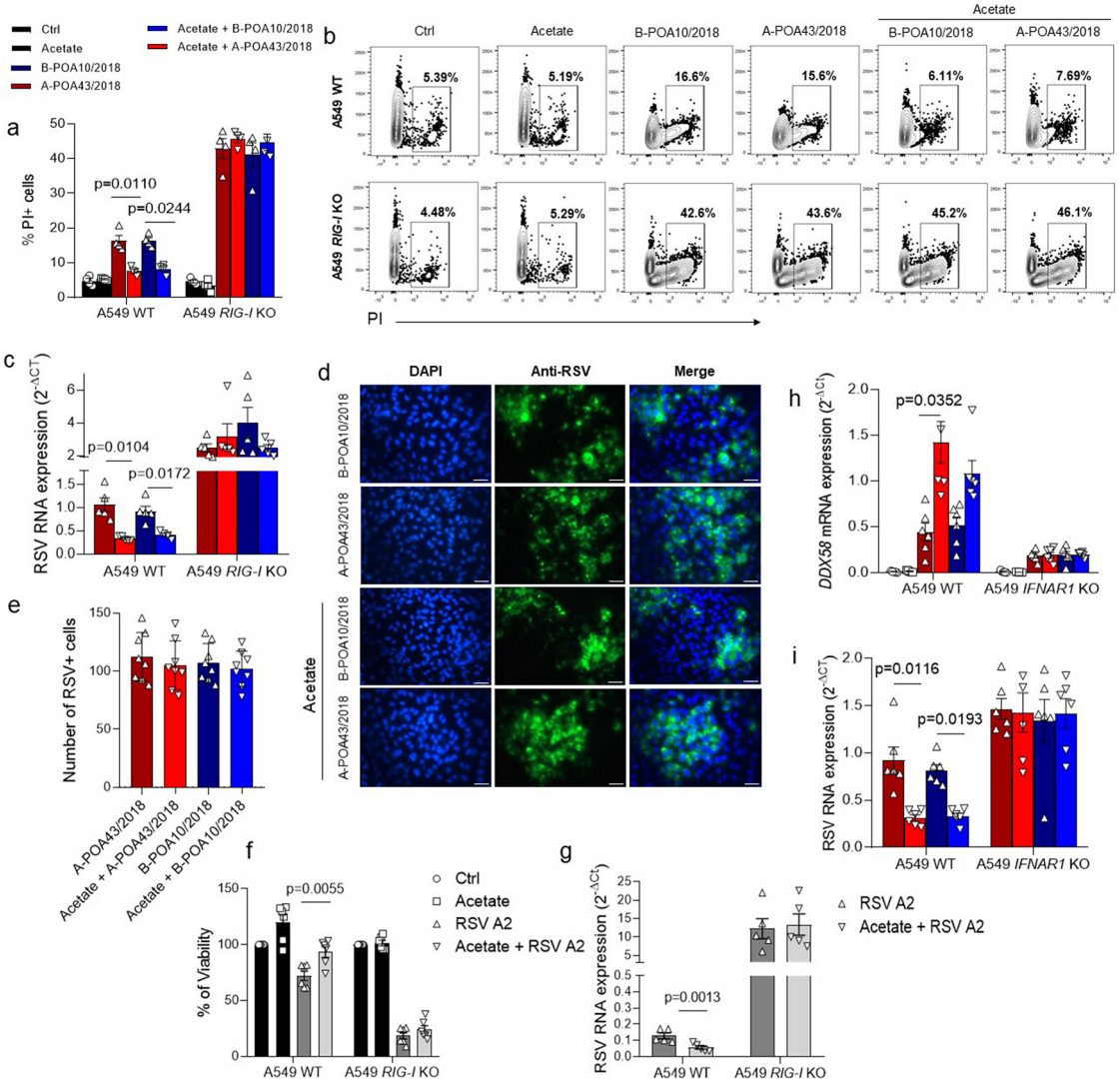


**Figure 2.** Acetate protection against RSV clinical isolates depends on RIG-I presence in human pulmonary cells. a–d, CRISPR/Cas9-generated RIG-I knockout (*RIG-I* KO) or wild-type (WT) A549 cells were pre-treated with 260 µM of acetate for 24 h and infected with $10^4$ PFU/ml (0.5 MOI) of clinical isolate RSV A-POA43/2018, B-POA10/2018 for 96 h or laboratory RSV strain A2 (f and g plots). a, Percent of PI (propidium iodide) positive cells detected by flow cytometry. b, Representative FACS profile of PI positive cells. Gating strategy is shown in appendix Figure 4. c, RSV F protein RNA levels detected using real-time PCR ($2^{-\Delta Ct}$). d, Fluorescence images of RSV (green) and cell nuclei using Hoescht (blue). Third panel shows data co-localization (merge). Scale bars = 60 µm. e, Immunofluorescence quantification measured by the number of RSV positive (green) cells. f, Percent of cell viability measured by MTT assay (using untreated/uninfected cells as viability control) in cells infected with RSA A2 strain. g, RSV F protein RNA levels detected using real-time PCR ($2^{-\Delta Ct}$) in cells infected with RSA A2 strain. h and i, CRISPR/Cas9-generated IFNAR1 knockout (*IFNAR1* KO) or WT A549 cells were pre-treated with 260 µM of acetate for 24 h and infected with $10^4$ PFU/ml of clinical isolate RSV A-POA43/2018 or B-POA10/2018 for 96 h or 24 h (h plot). h, DDX58 gene expression calculated using real-time PCR ($2^{-\Delta Ct}$). i, RSV F protein RNA levels calculated using real-time PCR ($2^{-\Delta Ct}$). Data are presented as mean ± SEM. All the experiments were performed in quadruplicates. The data are representative of 3 independent experiments, except in f to i, where 2 independent experiments were performed. Statistical significance between groups was determined with Kruskal–Wallis. A *p*-value lower than 0.05 was considered as significative.

infection (Figure 3, a). Mice treated with 20 $\mu$M SCFA-acetate significantly recovered their weight after acute RSV A-POA43/2018 infection (Figure 3, b). We also treated mice with 10 $\mu$M and found similar results (Supplementary Fig. E1). Five days after infection, fewer cells were found in the bronchoalveolar fluid of mice treated with SCFA-acetate, mainly on macrophage amount (Figure 3, c). Moreover, this reduction on cellularity was confirmed by diminished inflammatory infiltrate in the airways (Figure 3, d, e). There was also a

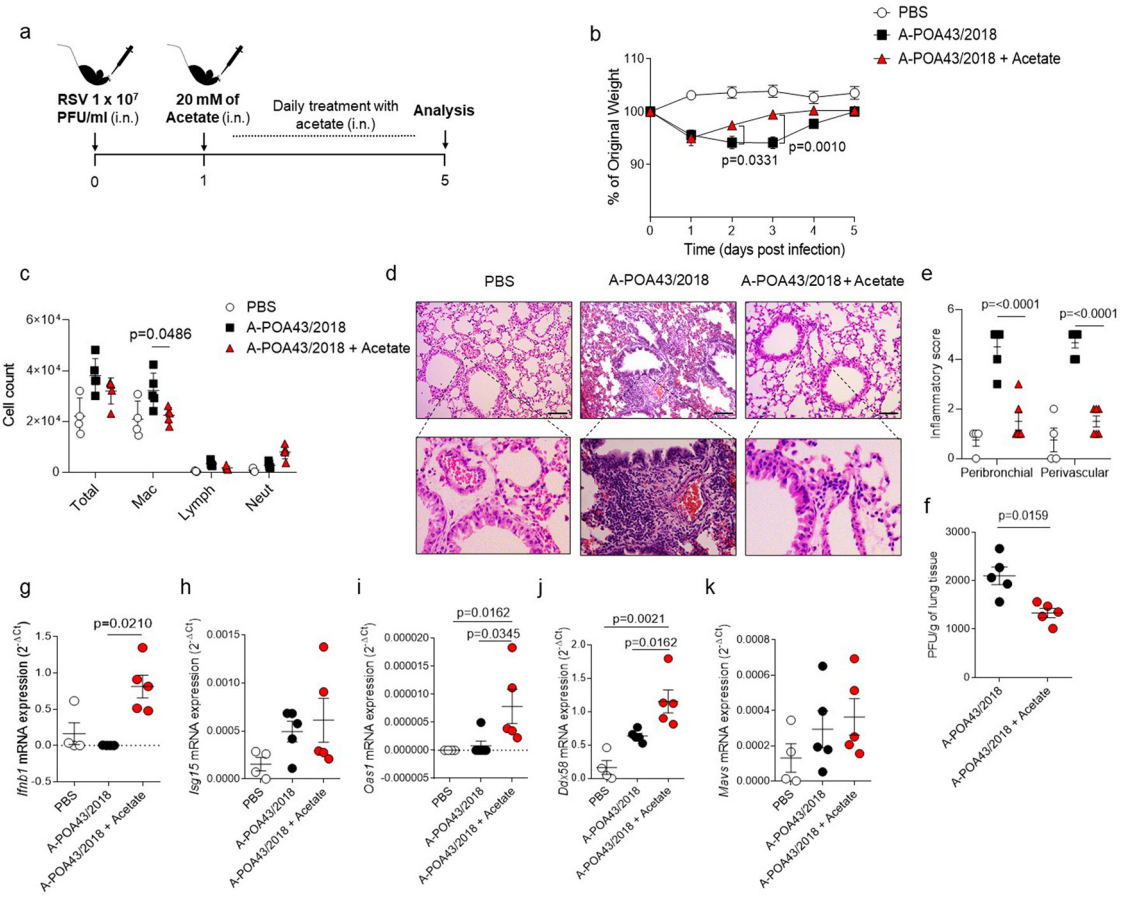


**Figure 3.** Intranasal acetate treatment protects against RSV clinical isolate infection *in vivo*. a, Experimental scheme. Female BALB/cJ mice were infected with clinical isolate RSV A-POA43/2018 ($10^7$ PFU/ml) and 24 h post infection treatment with 20 mM (40 $\mu$l) of acetate started through the intranasal route and PBS was administered as vehicle control. Treatment was performed daily up to 5 days after infection. b, Percentage body weight loss post infection relative to initial weight (day 0) ($n$ = 5). c, Total cell number and differential cell counts in bronchoalveolar lavage fluid. d, Representative images of lung tissue section stained with hematoxylin and eosin (H&E). Scale bars = 100 $\mu$m. e, H&E respective inflammation scores ($n$ = 3). f, Viral titre in the lung (PFUs/g lung tissue). g–k, *Ifnb1*, *Isg15*, *Oas1*, *Ddx58* and *Mavs* gene expression in the lung detected by real-time PCR ($2^{-\Delta Ct}$). The data are representative of 2 independent experiments. Data are presented as mean ± SEM. Statistical significance between groups was determined with Kruskal–Wallis, except in *F*, in which Mann–Whitney was used. A *p*-value lower than 0.05 was considered as significative.

significant reduction in the RSV viral load in the lung of animals treated with SCFA-acetate (Figure 4, f and appendix Figure 1 p 10). SCFA-acetate treatment increased *Ifnb1*, RIG-I and *Oas1* expression in the lung, but not *Mavs* expression (Figure 3, g–k). Thus, these data indicate a therapeutic effect of SCFA-acetate in the disease.

### Gut microbiota and stool acetate are associated with RSV bronchiolitis severity

After confirming that SCFA-acetate has a protective and resolving effect on infection with RSV isolated, we pursued to investigate the influence of this SCFA on children with bronchiolitis. We performed a screening with patients with RSV bronchiolitis where we sought to correlate the intestinal microbiota and the levels of acetate produced by it and to correlate with disease severity parameters. Of 45 infants who were hospitalized with symptoms suggestive of bronchiolitis during the study period, 30 were positive for RSV and negative for other viral pathogens. Therefore, these were recruited into the study. Demographic and clinical characteristics of the study population are shown in Table 1; the median age was 3 months, with a gestational age of 37 weeks; 70% were male, and 60% were Caucasian. The mean length of hospital stay was 5.7 days, and supplementary oxygen was administered for a mean of 2.7 days.

Stools from 17 infants were collected and used for microbial communities' analysis with 16S rRNA gene sequencing and quantification of SCFA. Microbiota composition differed markedly between individual

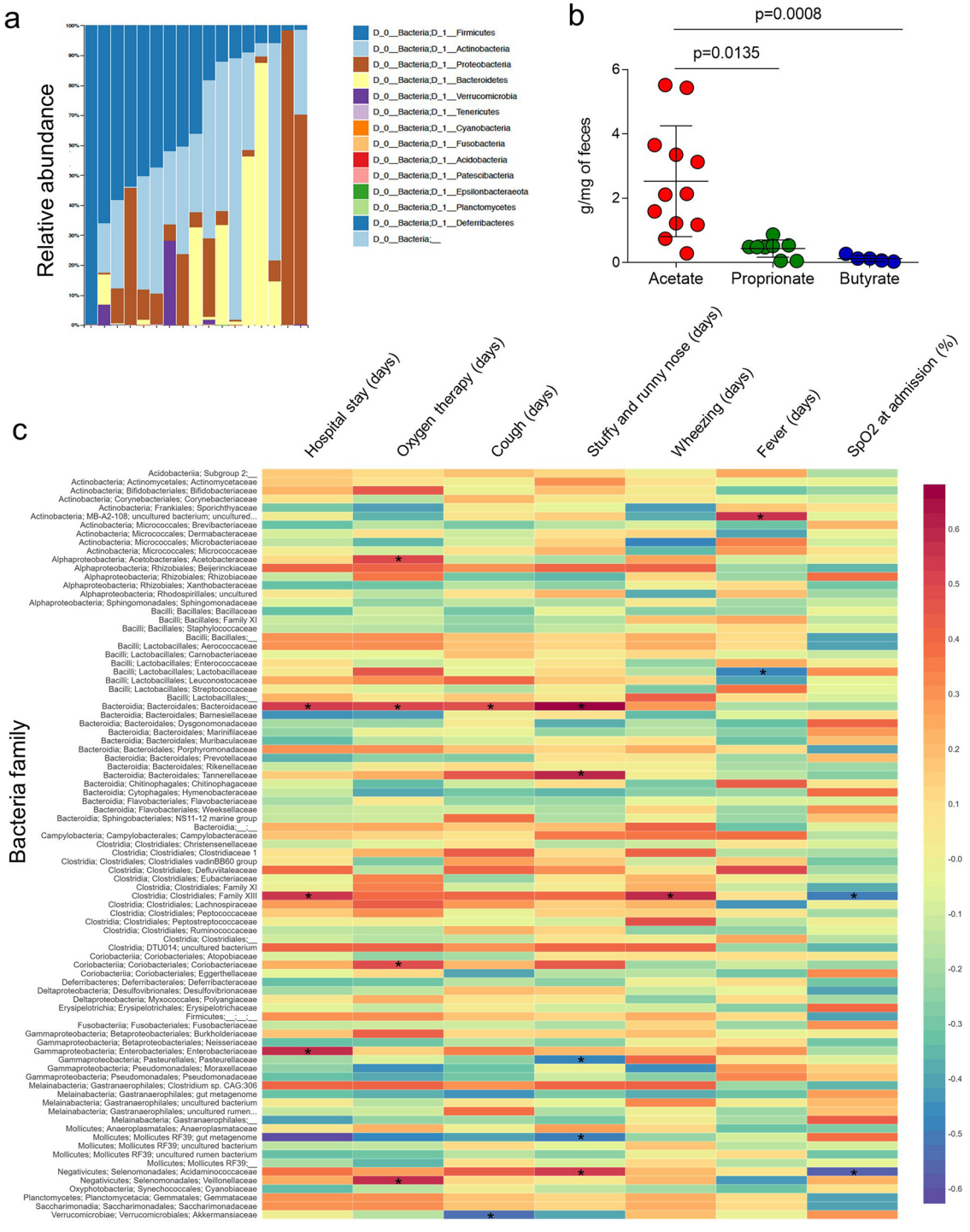


**Figure 4.** Gut microbiota composition and production of SCFA are associated with the severity of RSV-infected infants. a, microbiota composition analysis at phylum level using 16S rRNA gene sequencing (relative abundance). b, SCFA quantification in feces. c, Heatmap showing associations between the bacteria family and clinical parameters. Correlations were made through Spearman's rank correlation coefficient. Data in b is presented as mean ± SEM. The data are from 13 patients collected throughout the study. In b statistical significance between groups was determined with Kruskal–Wallis. A *p*-value lower than 0.05 was considered as significative.

| Variables | Values |
|---|---|
| Gender, mo, *n* (%) | |
| *Male* | 21 (70) |
| Age, mo (mean ± SD) | 3.20 ± 2.26 |
| Birth weight, *g* (mean ± SD) | 3034 ± 833.3 |
| Current weight, *g* (mean ± SD) | 5569 ± 1750 |
| Gestational age, mo (mean ± SD) | 37.40 ± 2.76 |
| Ethnicity, *n* (%) | |
| *Caucasian* | 18 (60) |
| *Afro-Brazilian* | 5 (16.7) |
| *Undeclared* | 7 (23.3) |
| Type of Delivery, *n* (%) | |
| *Vaginal* | 16 (53.3) |
| Gestational diabetes, *n* (%) | 3 (10) |
| Breastfeeding, *n* (%) | 20 (66.7) |
| Length of hospital stay, days (mean ± SD) | 5.69 ± 5.85 |
| $SpO_2$, %, (mean ± SD) | 97.55 ± 2.88 |
| $O_2$ need, days (mean ± SD) | 2.72 ± 2.47 |
| Fever, days (mean ± SD) | 1.93 ± 2.33 |
| Cough, days (mean ± SD) | 5.62 ± 4.91 |
| Stuffy/runny nose, days (mean ± SD) | 4.96 ± 3.78 |
| Wheezing, days (mean ± SD) | 2.38 ± 3.12 |
| Number of residents in the house (mean ± SD) | 4.89 ± 1.97 |

***Table 1*: Demographic and clinical characteristics of the RSV infected infant population.**
Definition of abbreviations: SD, standard deviation; g, grams; mo, months; CI, confidence interval. †Amounts calculated using the minimum wage in Brazil in 2018.

children (Figure 4, a). Acetate levels in feces were significantly higher compared to propionate and butyrate (Figure 4, b). Specific bacterial families in fecal microbiota were significantly correlated with acetate, propionate, and butyrate levels (Table 2), with a significant association between family *Dysgonomonadaceae* and acetate in stool. There were no correlations between SCFA levels and other bacterial families (Supplementary Table E2).

Gut microbial profile was associated with the severity of bronchiolitis (Figure 4, c): family *Bacteriodaceae* (phylum *Bacteroidetes*, class *Bacteroidia*) was positively associated with length of hospitalization (LOH), and the longer duration of cough and nasal congestion; in contrast, the genus *Mollicutes* RF39 (phylum *Tenericutes*) was inversely correlated with LOH.

Table 3 shows the relationship between acetate levels in faeces and clinical parameters. Increasing levels of acetate were significantly associated with increasing oxygen saturation at admission, and fewer days of fever. We observed no significant association between acetate levels in stools and breastfeeding (Supplementary Fig. E2, a, b, c). These data indicate that the infant gut microbiota and the acetate produced by it are associated with RSV bronchiolitis severity, leaning towards a profile that points to a mild disease.

### *Ex-vivo* treatment of nasopharyngeal aspirate cells with SCFA-acetate reduces RSV load and expression of ISGs

Since we found that acetate levels are associated with mild disease and the therapeutic treatment with it protects against infection with RSV clinical isolates, we decided to explore that further. We then investigated whether SCFA-acetate treatment of cells obtained from nasopharyngeal aspirates of patients with RSV bronchiolitis directly affects the viral load and expression of antiviral genes in these cells. In this model, treatment with SCFA-acetate significantly reduced RSV viral load compared to untreated cells of the infants, without interfering with cell viability (Figure 5, a, b, and Supplementary Fig. E2, d). There was no significant difference in the expression of the *IFNB1* (Figure 5, c); however, SCFA-acetate treatment significantly increased the expression of *OAS1* and *ISG15* (Figure 5, d, e). In addition, SCFA-acetate significantly increased the expression of virus recognition receptors MAVS and RIG-I (Figure 5, f, g). SCFA-acetate treatment did not modulate *TLR4* expression, which is associated with recognition the RSV protein F (Figure 5. h). As expected,

| Bacteria family | Positively correlated | | Negatively correlated | | SCFA |
|---|---|---|---|---|---|
| | *r* value | *p* value | *r* value | *p* value | |
| *Micrococcaceae* | | | -0.600* | 0.011 | Butyrate |
| | | | -0.535* | 0.027 | Propionate |
| *Dysgonomonadaceae* | 0.704** | 0.002 | | | Acetate |
| *Hymenobacteraceae* | 0.507* | 0.038 | | | Butyrate |
| Bacillales; *Family XI* | | | -0.537* | 0.026 | Propionate |
| *Lachnospiraceae* | 0.864*** | 0.000 | | | Propionate |
| *Sphingomonadaceae* | 0.495* | 0.043 | | | Butyrate |
| *Desulfovibrionaceae* | 0.518* | 0.033 | | | Butyrate |

***Table 2*: Correlation between fecal microbiota composition at the family level and SCFA quantification in faces.**
* $p < .05$; ** $p < .01$; *** $p < .001$.

| SCFA | Hospital stay (days) | Oxygen therapy (days) | $SpO_2$ at admission (%) | Fever (days) | Cough (days) | Blocked nose (days) | Wheezing (days) |
|---|---|---|---|---|---|---|---|
| **Acetate** | | | | | | | |
| $r_s$ value | -0.239 | -0.421 | 0.646 | -0.354 | -0.077 | -0.549 | -0.109 |
| *p* value | 0.410 | 0.133 | 0.026 | 0.027 | 0.775 | 0.063 | 0.640 |

***Table 3*: Correlation between SCFA quantification in faeces and clinical parameters (*n* = 12).**
$r_s$, Spearman correlation coefficient.

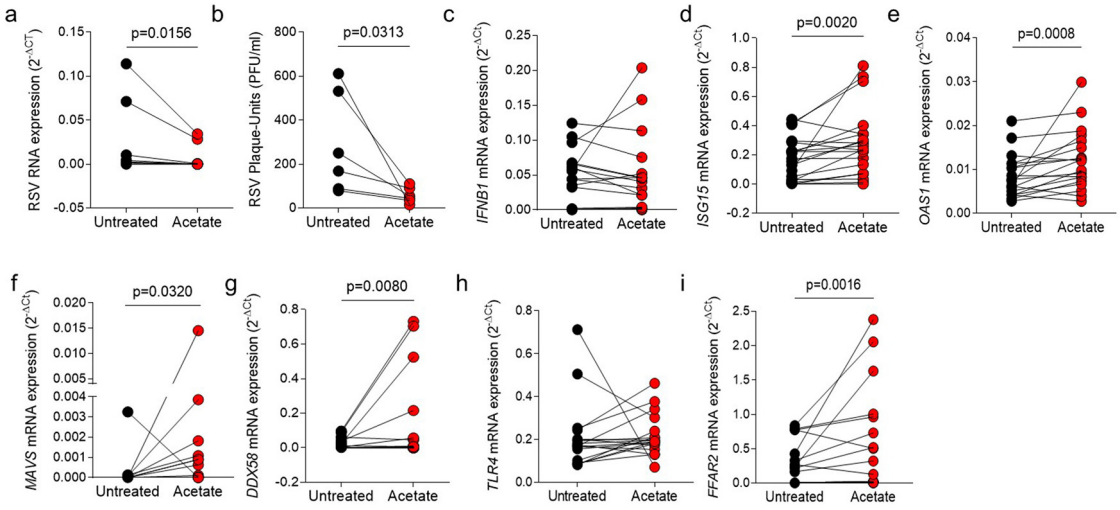


**Figure 5.** SCFA-acetate treatment reduces viral load and increases expression of antiviral molecules in cells from nasal washes of patients with RSV-bronchiolitis. d–i, Cells from nasopharyngeal washes of infants with RSV bronchiolitis were treated with 260 µM of SCFA-acetate for 24 h and then harvested for analysis. a, Real-time PCR analysis of RSV protein F gene expression detected by real-time PCR ($2^{-\Delta Ct}$). b, Viral plaque-assay (PFU/ml) performed using the supernatant. c-g, *IFNB1*, *ISG15*, *OAS1*, *DDX58* (RIG-I gene), and *MAVS* expression detected by real-time PCR ($2^{-\Delta Ct}$). h and i, *TLR4* and *FFAR2* (GPR43) expression detected by real-time PCR ($2^{-\Delta Ct}$) Data are presented as mean ± SEM. The data are from 7 to 30 patients collected throughout the study. From a to i the difference between the treatment and its untreated control was accessed by Wilcoxon matched-pairs signed rank test. A *p*-value lower than 0.05 was considered as significative.

treatment with SCFA-acetate significantly increased the expression of their specific receptor FFAR2 (Figure 5, i).

### The antiviral effect of SCFA-acetate through RIG-I induction is specific to RSV

We performed an *in vitro* analysis in lung epithelial cell lineage Calu-3, where we pretreated these cells with SCFA-acetate and infected with SARS-CoV-2 (0.1 MOI). We found that although SCFA-acetate was able to reduce the virus N1 gene expression at higher concentration (Figure 6, a), we did not observe difference on angiotensin-converting enzyme 2 (ACE2) expression, protein which has a role as entry receptor for SARS-CoV-2 to get into the host cell (Figure 5, b). In this model, SCFA-acetate did not increase ISG15, RIG-I or MDA5 (*IFIH1*) expression, once increased in RSV infection (Figure 6, c–e). To verify whether SCFA-acetate effect is specific to RSV we used the same experimental approach in nasopharyngeal aspirate samples from patients with COVID-19. In contrast to RSV findings, treatment with SCFA-acetate did not reduce SARS-CoV-2 viral titre (Figure 6, f). To address whether acetate is also modulating RSV infection and RIG-I expression in Calu-3 cells, we performed the same set of experiments using one of the RSV clinical strains in these cells. Similar to what we found in A549 cells, acetate reduced RSV levels and improved RIG-I expression in Calu-3 (Figure 6, g, h). These results suggests that SCFA-acetate treatment has a different protective effect on RSV mediated by RIG-I, reducing viral load and increasing antiviral genes in cells from patients already established RSV infection.

## Discussion

A series of studies presented herein provide new information about the role of the gut microbiota short-chain

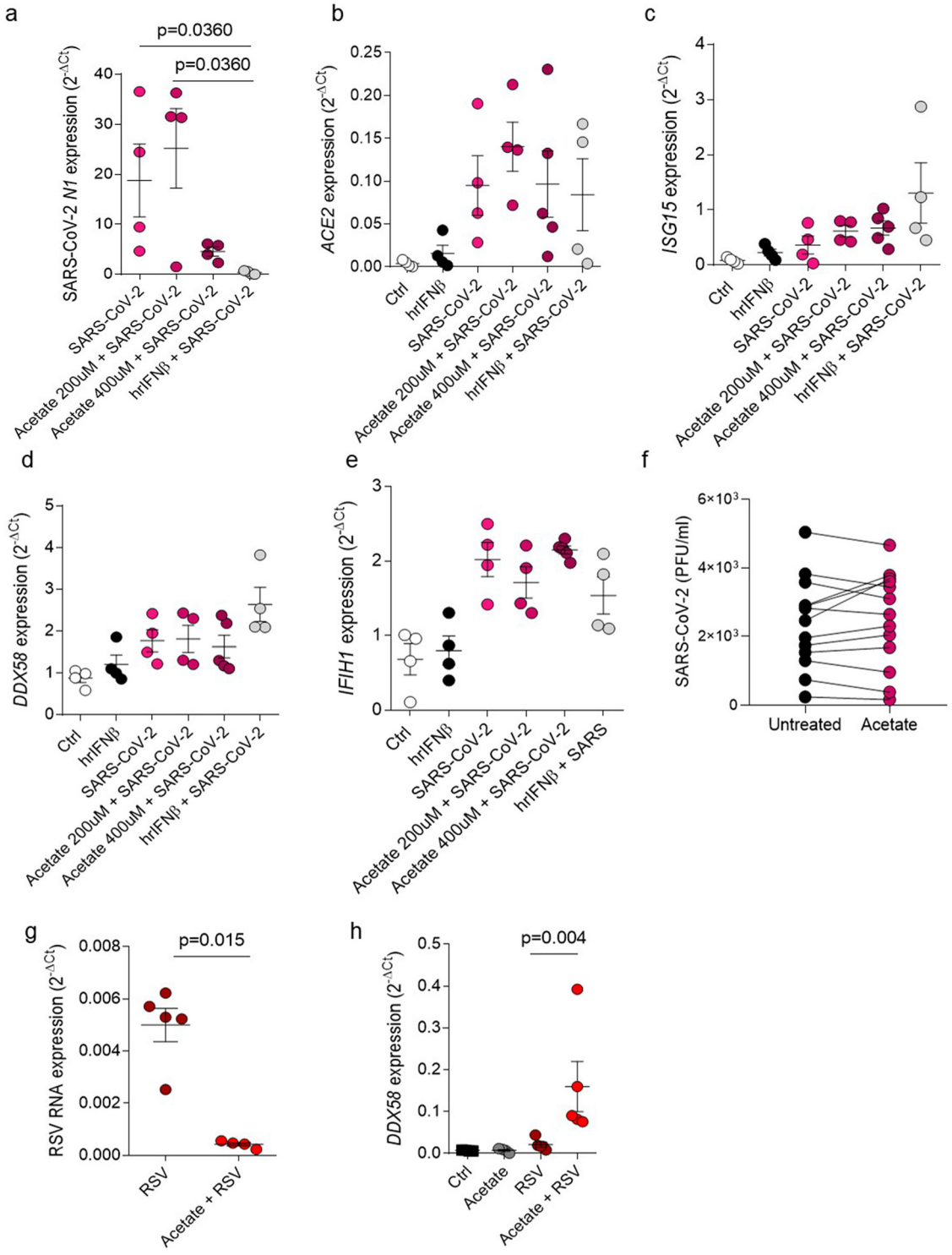


**Figure 6.** Acetate treatment does not have influence on SARS-CoV-2 infection. a–d, Calu-3 cells were pre-treated with 200 µM or 400 µM of acetate for 24 h or pre-treated with 100 UI of human recombinant IFN$\beta$ for 6 h. Cells were then infected with 0.1 MOI (multiplicity of infection) of SARS-CoV-2 and left in culture for 2 days. a, SARS-CoV-2 *N1* (virus nucleocapsid) gene expression detected by real-time PCR ($2^{-\Delta Ct}$). b-e, *ACE2, ISG15, DDX58* (RIG-I) gene expression detected by real-time PCR ($2^{-\Delta Ct}$). f, viral plaque-assay (PFU) of cells from nasopharyngeal aspirate samples from patients with SARS-CoV-2 treated with 260 µM of acetate for 24 h (PFU/ml). g,h, Calu-3 cells were pre-treated with 260 µM of acetate for 24 h and infected with $10^4$ PFU/ml (0.5 MOI) of clinical isolate

fatty acid SCFA-acetate in modulating the severity of RSV-associated lower respiratory illness. Although we have already shown that SCFA-acetate protects against RSV in a GPR43- and IFNAR-dependent manner,[24] in this work we have moved forward in a translational manner, showing protection against RSV viral isolates and in samples from children with bronchiolitis. The present study investigated the role of RIG-I in the mediating the antiviral response of SCFA-acetate. Also, we highlighted the importance of the SCFA-acetate direct antiviral effects in the respiratory tract and therapeutic after infection. Moreover, we have shown the effects of SCFA-acetate treatment against another important and heavily investigated respiratory virus, SARS-CoV-2.

The importance of acetate has also been demonstrated during influenza infection in mice for protection against the secondary pulmonary pneumococcal superinfection.[34] Also, acetate protects against lung infection of Klebsiella pneumoniae[35]

*In vitro* model using human pulmonary epithelial cells showed a clear protective effect of pre-treatment with acetate against infection with clinical RSV isolates. In a mechanistic study using RIG-I knockout human pulmonary epithelial cells we have shown that protective effect of acetate against RSV infection relies on RIG-I presence. RIG-I is well known as a key sensors of virus infection, being one of the germline-encoded patterns-recognition receptors (PRR).[36,37] Additionally, RIG-I directly inhibits viral replication independent of antiviral signalling.[38] In our study we found that RIG-I is playing a pivotal role as ISG in the context of acetate treatment. This is due to the loss of effect on the expression of RIG-I by acetate in the absence of IFNAR1. Although other ISGs such as OAS1 have shown an effect in directly regulating RSV replication, our study suggests that RIG-I may also have a direct antiviral role, as the virus replicates more in RIG-I knockout cells than in absence of IFNAR1. Previous studies confirmed the important role of RIG-I during RSV infection, a study has shown that the absence of RIG-I can dramatically reduce IFN-$\beta$ and ISG15 expression levels during RSV infection, turning into an important molecule for antiviral response in this situation.[39] Also, *Mavs*$^{-/-}$ mice, unable to signal via MDA-5 or RIG-I, failed in induce type I IFN and activate neutrophils in the lung during the disease caused by RSV.[40] Thus, it is clear the antiviral role played by RIG-I throughout RSV infection, and this may partially explain the fact that the virus specifically inhibits this signalling pathway. RSV and its non-structural proteins (NS) interact indirectly with RIG-I, inhibiting it, as part of its antiviral response evasion mechanism. For example, RSV NS1 interacts with TRIM25 and interferes with RIG-I ubiquitination to suppress type-I interferon signalling.[41] Although the protection of acetate pre-treatment *in vitro* was dependent on RIG-I for both clinical isolates, we just found a significant expression of ISGs expression mediated by acetate with the RSV subtype A (A-POA43/2018). Other studies previously demonstrated the difference in the ISGs expression levels between the RSV subtypes.[42] Consequently, we choose the A-POA43/2018 isolate to continue to investigate the effect of acetate *in vivo*.

In our study the effectiveness of the treatment with acetate following RSV infection with clinical RSV strains isolated from infants hospitalized for RSV bronchiolitis was then confirmed *in vivo* in a mouse model where the RIG-I expression was also induced. Animals treated with acetate recovered significantly faster, with a significant reduction in the RSV viral load in the lung. *Ex vivo* studies using respiratory epithelial cells collected from RSV infected patients by nasopharyngeal aspirates demonstrated that treatment of RSV-infected cells with acetate decreases RSV viral load and increases interferon-stimulated gene expression, highlighting to a robust RIG-I induction. Conversely, we did not find a significant increase in *IFNB1* expression or IFN-$\beta$ production in cells exposed to acetate treatment we performed the analysis 24 h after acetate treatment. One relevant explanation for that may be timing for detection of type I IFNs, which usually peaks for a short period after infection.[33] Also, the IFN-$\beta$ production was undetected in the nasopharyngeal aspirate of the patients. According, a study using nasal epithelial cells from children with wheezing and/or atopy found a reduced production of IFN-$\beta$ in response to RSV infection, which was associated with increased viral shedding[43,44]

In the study of infants hospitalized with RSV bronchiolitis, we have shown that specific bacterial strains in gut microbiota are associated with differing levels of short-chain fatty acids (including acetate), and that increasing levels of acetate in feces were associated with better clinical outcomes, including higher oxygen saturation levels at hospital admission and shorter duration of fever.

We have shown that different families in gut microbiota likely elicit specific clinical effects in relation to RSV infection. For example, *Bacteriodaceae* family was significantly associated with a worse severity profile,

RSV A-POA43/2018 for 96 h (g) or 24 h (h). g, RSV F protein RNA levels calculated using real-time PCR ($2^{-\Delta Ct}$). h, *DDX58* gene expression assessed using real-time PCR ($2^{-\Delta Ct}$). Data are presented as mean ± SEM. All the experiments were performed in quadruplicates. The data are representative of 2 independent experiments. Data in e is from 13 patients. Statistical significance between groups was determined with Kruskal–Wallis, except in f, where the difference between the treatment and its untreated control was accessed by Wilcoxon matched-pairs signed rank test. In g Mann–Whitney was used to determine the difference between the groups. A *p*-value lower than 0.05 was considered as significative.

similar to what has been reported previously.[45] Previous studies have reported an increase in *Clostridiales* colonies in the gut microbiota of RSV-infected patients.[19] In our study, we observed a correlation of this family with increased duration of hospitalization and wheezing, suggesting a possible association with disease severity. In contrast, the presence of genus *Mollicutes*/RF39 appeared protective. Interestingly, this genus has been shown to protect against early intestinal frailty, improve gut integrity and increase SCFA production.[46]

Other SFCA (butyrate and propionate) are usually found in lower concentrations in the gut/stools,[47] and were mostly undetected in our study. A study showed that acetate was the SCFA with highest concentrations in infant's gut, and that it is strongly influenced by breastfeeding.[48] Breastfeeding is also known to be associated with lower risk for severe RSV infection, with a probable protective role for respiratory infections by other viruses as well.[49–51] In our study, there was no association between acetate levels and breastfeeding, but we recruited only infants with moderate/severe RSV bronchiolitis and have shown that acetate was protective against clinically severe RSV infections. We therefore cannot exclude the possibility that protection afforded by breastfeeding may be in part mediated by the effect on gut microbiota and higher acetate levels, none of the infants included in the study were under complementary feeding.

The human studies have some limitations. We choose to exclude patients under antibiotic treatment, to due the microbiota analysis, consequently the use of antibiotic limited the number of patients recruited for the study of RSV bronchiolitis. We did not analyze the presence of all respiratory virus in the nasopharyngeal samples. Another limitation is that we did not have access to the feces for microbiome analysis of all recruited patients and we did not evaluate the nasopharyngeal microbiome. Recent studies have shown that the nasopharyngeal microbiome is associated with severe early-life acute respiratory infections by RSV and risk of asthma development.[52–54] In the present study we aimed to measure the SCFA production in the lung as they show to be related to inflammatory markers in viral bronchilitis.[55] However, due to a limitation in our methodology, we were unable to detect SCFA production in the nasal washes of the infants, which would bring more robust conclusions to the study. A previous study showed that the levels of acetate in the nasal secretion are not different from children with viral bronchiolitis comparing to non-viral bronchiolitis.[55] There is evidence that SCFA can be found in the airways as result of lung microbiome metabolism.[56] However, some studies suggest that the major source of SCFA in the lung are from gut microbiota,[57] underlining the importance of our findings on acetate levels in the feces of RSV-infected children and the association with the clinical outcomes.

In our study we also investigate the role of acetate in control SARS-CoV-2 infection in pulmonary cells lines. Although acetate pre-treatment reduced the SARS-CoV-2 viral load in Calu-3 cells, it did not induce RIG-I expression, even in the higher dose than used in the RSV analysis, highlighting the difference in the effect of acetate on these two viruses. One possibility is that acetate might be decreasing viral detection without impacting on virus production. Future *in vivo* studies using acetate pre-treatment might confirm the prophylactic effect of acetate against SARS-CoV-2 infection. Also, the acetate effect in reducing viral load after infection seems to be effective towards RSV as we did not find the same outcome in SARS-CoV-2 infection in nasopharyngeal cells from infected patients. It is important to notice that children display higher basal expression of MDA5 and RIG-I in upper airway epithelial cells, macrophages, and dendritic cells, resulting in stronger innate antiviral responses upon SARS-CoV-2 infection than in adults.[58] Thus, acetate may be acting through a different mechanism than that one presented in infection and bronchiolitis caused by RSV. In agreement to our findings with previous SARS-CoV-2-infected nasopharyngeal cells, a study showed that SCFA treatment did not interfere with SARS-CoV-2 infection in human intestinal biopsies and intestinal epithelial cells.[59]

Several studies have been suggestion the trigger of the tissue immune response as answer for many infections disease,[60] and here we show the importance of acetate, a gut microbiota metabolite, in the respiratory tract to control RSV infection. Our data suggest that acetate can be considered as a viable intervention to control or prevent severe RSV lower respiratory tract infection. Future clinical trials should confirm whether the use of acetate is effective in this context. Taken together, our results indicate that acetate mechanism of action is through modulation of RIG-I expression significantly reducing RSV viral load.

## Contributors

A.P.D.S., R.S., M.A.R.V., and K.H.A. conceived the study and designed the experiments. A.P.D.S., R.S., M.A.R.V., and K.H.A verified the underlying data. K.H.A., C.M.F., E.F.S. and D.N.F. recruited and enrolled the infants to the study. J.S., M.M. and L.L. collected the nasal washes samples. K.H.A., C.M.F., E.F.S. and D.N.F. performed the ex vivo SCFA treatment on the cells from nasal washes. K.H.A. and C.M.F. processed the samples and carried out the RT-PCR analysis. K.H.A., J.L.F. and L.P.P. performed the *in vivo* experiments. A.G. and L.D. performed the isolation of virus from clinical samples. S.O. and H.R. performed the SCFA quantification in stool samples. G.C., J.I.B.G., T.M.R., B.L.A., M.D., N.D.M.S., C.V.B, P.M. and L.A.B. contributed to SARS-CoV-2 analysis. M.R., S.G., J.C.S., F.Q.M. and A.P.M.V. did the microbiota analysis and interpretation.

T.R.J. and D.S.M. generated A549 RIG-I and IFNAR1 KO cells and contributed to data interpretation. M.H.J., M.E., F.P.P., A.C. and R.S. contributed to clinical and statistical analysis and data interpretation. A.P.D.S., R. S. and M.A.R.V. supervised and designed all the study. A.P.D.S., R.S., M.A.R.V., A.C. and K.H.A. wrote the manuscript. All authors read and approved the final version of the manuscript.

## Data sharing statement

All primary data in this study will be made available upon request to the corresponding authors for individuals with appropriate data sharing agreements in place.

## Declaration of interests

The authors declare no competing interests.

## Acknowledgments

We thank Rodrigo Dorneles for technical assistance. This study was supported by Rio Grande do Sul Research Foundation FAPERGS (FAPERGS/MS/CNPq/SESRS no. 03/2017 - PPSUS 17/2551-0001380-8 and COVID-19 20/2551-0000258-6), CNPq 312504/2017-9 and by Coordenação de Aperfeiçoamento de Pessoal de Nível Superior - Brasil (CAPES) - Finance Code 001. P.B., C.V.B. and L.A.B. would like to acknowledge financial support given by CNPq/FAPERGS/CAPES/BNDES to the National Institute of Science and Technology on Tuberculosis (INCT-TB), Brazil [grant numbers: 421703-2017-2/17-1265-8/14.2.0914.1). This study was also supported by research grant from Fundação de Amparo à pesquisa do estado de São Paulo (FAPESP) no. 18/15313-8 and 20/04583-4. J.L.F. and L.P.P. are recipients of fellowships from FAPESP no. 2017/06577-9 and no. 2020/13689-0, respectively.

## Supplementary materials

Supplementary material associated with this article can be found in the online version at doi:10.1016/j.ebiom.2022.103891.

### References

1 Nair H, Nokes DJ, Gessner BD, et al. Global burden of acute lower respiratory infections due to respiratory syncytial virus in young children: a systematic review and meta-analysis. *Lancet*. 2010;375(9725):1545–1555.
2 Shi T, McAllister DA, O'Brien KL, et al. Global, regional, and national disease burden estimates of acute lower respiratory infections due to respiratory syncytial virus in young children in 2015: a systematic review and modelling study. *Lancet*. 2017;390(10098):946–958.
3 Foley DA, Phuong LK, Englund JA. Respiratory syncytial virus immunisation overview. *J Paediatr Child Health*. 2020;56(12):1865–1867.
4 Mazur NI, Higgins D, Nunes MC, et al. The respiratory syncytial virus vaccine landscape: lessons from the graveyard and promising candidates. *Lancet Infect Dis*. 2018;18(10):e295–e311.
5 Ruckwardt TJ, Morabito KM, Graham BS. Immunological lessons from respiratory syncytial virus vaccine development. *Immunity*. 2019;51(3):429–442.
6 Polack FP, Stein RT, Custovic A. The syndrome we agreed to call bronchiolitis. *J Infect Dis*. 2019;220(2):184–186.
7 Raita Y, Camargo CA, Bochkov YA, et al. Integrated-omics endotyping of infants with rhinovirus bronchiolitis and risk of childhood asthma. *J Allergy Clin Immunol*. 2021;147(6):2108–2117.
8 Thorburn AN, McKenzie CI, Shen S, et al. Evidence that asthma is a developmental origin disease influenced by maternal diet and bacterial metabolites. *Nat Commun*. 2015;6:7320.
9 Friedrich L, Pitrez PM, Stein RT, Goldani M, Tepper R, Jones MH. Growth rate of lung function in healthy preterm infants. *Am J Respir Crit Care Med*. 2007;176(12):1269–1273.
10 Habibi MS, Thwaites RS, Chang M, et al. Neutrophilic inflammation in the respiratory mucosa predisposes to RSV infection. *Science*. 2020;370(6513):eaba9301. https://doi.org/10.1126/science.aba9301.
11 Schoggins JW, Wilson SJ, Panis M, et al. A diverse range of gene products are effectors of the type I interferon antiviral response. *Nature*. 2011;472(7344):481–485.
12 Wark PA, Johnston SL, Bucchieri F, et al. Asthmatic bronchial epithelial cells have a deficient innate immune response to infection with rhinovirus. *J Exp Med*. 2005;201(6):937–947.
13 Ling Z, Tran KC, Teng MN. Human respiratory syncytial virus nonstructural protein NS2 antagonizes the activation of beta interferon transcription by interacting with RIG-I. *J Virol*. 2009;83(8):3734–3742.
14 Spann KM, Tran KC, Chi B, Rabin RL, Collins PL. Suppression of the induction of alpha, beta, and lambda interferons by the NS1 and NS2 proteins of human respiratory syncytial virus in human epithelial cells and macrophages [corrected]. *J Virol*. 2004;78(8):4363–4369.
15 Boyapalle S, Wong T, Garay J, et al. Respiratory syncytial virus NS1 protein colocalizes with mitochondrial antiviral signaling protein MAVS following infection. *PLoS One*. 2012;7(2):e29386.
16 Melero JA, Moore ML. Influence of respiratory syncytial virus strain differences on pathogenesis and immunity. *Curr Top Microbiol Immunol*. 2013;372:59–82.
17 Stokes KL, Chi MH, Sakamoto K, et al. Differential pathogenesis of respiratory syncytial virus clinical isolates in BALB/c mice. *J Virol*. 2011;85(12):5782–5793.
18 Villenave R, O'Donoghue D, Thavagnanam S, et al. Differential cytopathogenesis of respiratory syncytial virus prototypic and clinical isolates in primary pediatric bronchial epithelial cells. *Virol J*. 2011;8:43.
19 Harding JN, Siefker D, Vu L, et al. Altered gut microbiota in infants is associated with respiratory syncytial virus disease severity. *BMC Microbiol*. 2020;20(1):140.
20 Groves HT, Cuthbertson L, James P, Moffatt MF, Cox MJ, Tregoning JS. Respiratory disease following viral lung infection alters the murine gut microbiota. *Front Immunol*. 2018;9:182.
21 Groves HT, Higham SL, Moffatt MF, Cox MJ, Tregoning JS. Respiratory viral infection alters the gut microbiota by inducing inappetence. *mBio*. 2020;11(1):e03236-19. https://doi.org/10.1128/mBio.03236-19.
22 McFarlane AJ, McSorley HJ, Davidson DJ, et al. Enteric helminth-induced type I interferon signaling protects against pulmonary virus infection through interaction with the microbiota. *J Allergy Clin Immunol*. 2017;140(4):1068–1078. e6.
23 Schaupp L, Muth S, Rogell L, et al. Microbiota-induced type I interferons instruct a poised basal state of dendritic cells. *Cell*. 2020;181(5):1080–1096. e19.
24 Antunes KH, Fachi JL, de Paula R, et al. Microbiota-derived acetate protects against respiratory syncytial virus infection through a GPR43-type 1 interferon response. *Nat Commun*. 2019;10(1):3273.
25 Aguiar JA, Tremblay BJ, Mansfield MJ, et al. Gene expression and *in situ* protein profiling of candidate SARS-CoV-2 receptors in human airway epithelial cells and lung tissue. *Eur Respir J*. 2020;56(3):2001123. https://doi.org/10.1183/13993003.01123-2020.
26 Laporte M, Raeymaekers V, Van Berwaer R, et al. The SARS-CoV-2 and other human coronavirus spike proteins are fine-tuned towards temperature and proteases of the human airways. *PLoS Pathog*. 2021;17:(4) e1009500.

27 Saccon E, Chen X, Mikaeloff F, et al. Cell-type-resolved quantitative proteomics map of interferon response against SARS-CoV-2. *iScience*. 2021;24:(5) 102420.
28 Thio CL, Chi PY, Lai AC, Chang YJ. Regulation of type 2 innate lymphoid cell-dependent airway hyperreactivity by butyrate. *J Allergy Clin Immunol*. 2018;142(6):1867–1883. e12.
29 Castro-Rodriguez JA, Rodrigo GJ, Rodriguez-Martinez CE. Principal findings of systematic reviews of acute asthma treatment in childhood. *J Asthma*. 2015;52(10):1038–1045.
30 McCallum GB, Morris PS, Wilson CC, et al. Severity scoring systems: are they internally valid, reliable and predictive of oxygen use in children with acute bronchiolitis? *Pediatr Pulmonol*. 2013;48 (8):797–803.
31 Rolfsjord LB, Skjerven HO, Carlsen KH, et al. The severity of acute bronchiolitis in infants was associated with quality of life nine months later. *Acta Paediatr*. 2016;105(7):834–841.
32 Pinto LA, Pitrez PM, Luisi F, et al. Azithromycin therapy in hospitalized infants with acute bronchiolitis is not associated with better clinical outcomes: a randomized, double-blinded, and placebo-controlled clinical trial. *J Pediatr*. 2012;161(6):1104–1108.
33 McCutcheon KM, Jordan R, Mawhorter ME, et al. The interferon type I/III response to respiratory syncytial virus infection in airway epithelial cells can be attenuated or amplified by antiviral treatment. *J Virol*. 2016;90(4):1705–1717.
34 Sencio V, Barthelemy A, Tavares LP, et al. Gut dysbiosis during influenza contributes to pulmonary pneumococcal superinfection through altered short-chain fatty acid production. *Cell Rep*. 2020;30(9):2934–2947. e6.
35 Galvao I, Tavares LP, Correa RO, et al. The metabolic sensor GPR43 receptor plays a role in the control of klebsiella pneumoniae infection in the lung. *Front Immunol*. 2018;9:142.
36 Rehwinkel J, Gack MU. RIG-I-like receptors: their regulation and roles in RNA sensing. *Nat Rev Immunol*. 2020;20(9):537–551.
37 Xu XX, Wan H, Nie L, Shao T, Xiang LX, Shao JZ. RIG-I: a multifunctional protein beyond a pattern recognition receptor. *Protein Cell*. 2018;9(3):246–253.
38 Chan YK, Gack MU. RIG-I works double duty. *Cell Host Microbe*. 2015;17(3):285–287.
39 Liu P, Jamaluddin M, Li K, Garofalo RP, Casola A, Brasier AR. Retinoic acid-inducible gene I mediates early antiviral response and Toll-like receptor 3 expression in respiratory syncytial virus-infected airway epithelial cells. *J Virol*. 2007;81(3):1401–1411.
40 Kirsebom FCM, Kausar F, Nuriev R, Makris S, Johansson C. Neutrophil recruitment and activation are differentially dependent on MyD88/TRIF and MAVS signaling during RSV infection. *Mucosal Immunol*. 2019;12(5):1244–1255.
41 Ban J, Lee NR, Lee NJ, Lee JK, Quan FS, Inn KS. Human respiratory syncytial virus NS 1 targets TRIM25 to suppress RIG-I ubiquitination and subsequent RIG-I-mediated antiviral signaling. *Viruses*. 2018;10(12):716. https://doi.org/10.3390/v10120716.
42 Pierangeli A, Viscido A, Bitossi C, et al. Differential interferon gene expression in bronchiolitis caused by respiratory syncytial virus-A genotype ON1. *Med Microbiol Immunol*. 2020;209 (1):23–28.
43 Spann KM, Baturcam E, Schagen J, et al. Viral and host factors determine innate immune responses in airway epithelial cells from children with wheeze and atopy. *Thorax*. 2014;69 (10):918–925.
44 Thwaites RS, Coates M, Ito K, et al. Reduced nasal viral load and IFN responses in infants with respiratory syncytial virus bronchiolitis and respiratory failure. *Am J Respir Crit Care Med*. 2018;198 (8):1074–1084.
45 Hasegawa K, Linnemann RW, Mansbach JM, et al. The fecal microbiota profile and bronchiolitis in infants. *Pediatrics*. 2016;138(1): e20160218. https://doi.org/10.1542/peds.2016-0218.
46 Jackson MA, Jeffery IB, Beaumont M, et al. Signatures of early frailty in the gut microbiota. *Genome Med*. 2016;8(1):8.
47 Differding MK, Benjamin-Neelon SE, Hoyo C, Ostbye T, Mueller NT. Timing of complementary feeding is associated with gut microbiota diversity and composition and short chain fatty acid concentrations over the first year of life. *BMC Microbiol*. 2020;20 (1):56.
48 Bridgman SL, Azad MB, Field CJ, et al. Fecal short-chain fatty acid variations by breastfeeding status in infants at 4 months: differences in relative versus absolute concentrations. *Front Nutr*. 2017;4:11.
49 Nishimura T, Suzue J, Kaji H. Breastfeeding reduces the severity of respiratory syncytial virus infection among young infants: a multicenter prospective study. *Pediatr Int*. 2009;51(6):812–816.
50 Oddy WH. A review of the effects of breastfeeding on respiratory infections, atopy, and childhood asthma. *J Asthma*. 2004;41 (6):605–621.
51 Roine I, Fernandez JA, Vasquez A, Caneo M. Breastfeeding reduces immune activation in primary respiratory syncytial virus infection. *Eur Cytokine Netw*. 2005;16(3):206–210.
52 Biesbroek G, Tsivtsivadze E, Sanders EA, et al. Early respiratory microbiota composition determines bacterial succession patterns and respiratory health in children. *Am J Respir Crit Care Med*. 2014;190(11):1283–1292.
53 Rosas-Salazar C, Shilts MH, Tovchigrechko A, et al. Nasopharyngeal microbiome in respiratory syncytial virus resembles profile associated with increased childhood asthma risk. *Am J Respir Crit Care Med*. 2016;193(10):1180–1183.
54 Teo SM, Mok D, Pham K, et al. The infant nasopharyngeal microbiome impacts severity of lower respiratory infection and risk of asthma development. *Cell Host Microbe*. 2015;17(5):704–715.
55 Lynch JP, Werder RB, Loh Z, et al. Plasmacytoid dendritic cells protect from viral bronchiolitis and asthma through semaphorin 4a-mediated treg expansion. *J Exp Med*. 2018;215(2):537–557.
56 Segal LN, Clemente JC, Li Y, et al. Anaerobic bacterial fermentation products increase tuberculosis risk in antiretroviral-drug-treated HIV patients. *Cell Host Microbe*. 2017;21(4):530–537. e4.
57 Liu Q, Tian X, Maruyama D, Arjomandi M, Prakash A. Lung immune tone via gut-lung axis: gut-derived LPS and short-chain fatty acids' immunometabolic regulation of lung IL-1beta, FFAR2, and FFAR3 expression. *Am J Physiol Lung Cell Mol Physiol*. 2021;321(1):L65–L78.
58 Loske J, Rohmel J, Lukassen S, et al. Pre-activated antiviral innate immunity in the upper airways controls early SARS-CoV-2 infection in children. *Nat Biotechnol*. 2021. https://doi.org/10.1038/s41587-021-01037-9.
59 Pascoal LB, Rodrigues PB, Genaro LM, et al. Microbiota-derived short-chain fatty acids do not interfere with SARS-CoV-2 infection of human colonic samples. *Gut Microbes*. 2021;13(1):1–9.
60 Farber DL. Tissues, not blood, are where immune cells function. *Nature*. 2021;593(7860):506–509.